The College of Engineering
University of Wisconsin-Madison

Wisconsin Electric Machines and Power Electronics Consortium

RESEARCH REPORT
93-23

Field Oriented Control of Synchronous Reluctance Machine

Takayoshi Matsuo and Thomas A. Lipo
Dept. of Electrical and Computer Engineering
University of Wisconsin-Madison
1415 Johnson Drive
Madison, WI 53706

WEMPEC

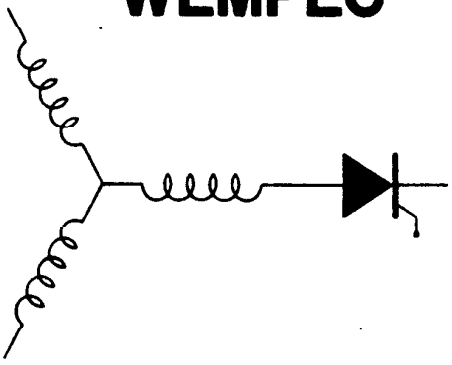

Department of Electrical and Computer Engineering
1415 Johnson Drive
Madison, Wisconsin 53706

Field Oriented Control of Synchronous Reluctance Machine

Takayoshi Matsuo and Thomas A. Lipo
University of Wisconsin-Madison
Electrical and Computer Engineering
1415 Johnson Drive
Madison, Wisconsin 53706

Abstract- In this paper, control strategies, practical implementation and performance issues related to field oriented control of synchronous reluctance motors are presented. In particular, a speed invariant current controller, variable d-q current limit and variable speed loop gain are proposed. Excellent control performance is shown to be possible, which indicates that synchronous reluctance motors can be suitably applied to high performance drive systems.

INTRODUCTION

The synchronous reluctance motor is one of the oldest types of electric motors and has, from time to time, attracted the efforts of a considerable number of investigators [1-3]. The synchronous reluctance motor is a singly salient machine in which the rotor is constructed so as to employ the principle of reluctance torque to produce electromechanical energy conversion. Only the rotor is constructed with salient poles while the stator inner surface is cylindrical and typically wound in an identical manner to that of an induction machine. Thus, the machine typically retains many of the benefits of variable reluctance motors while at the same time eliminating several of its disadvantages. The noise and torque pulsation problems, so difficult to overcome with variable (switched) reluctance motors, can be elegantly overcome in a synchronous reluctance machine by simply winding the stator in the conventional manner so as to produce a sinusoidal uniformly rotating air gap MMF.

It is the purpose of this paper to propose and examine the control strategies related to synchronous reluctance motors as a possible alternative for ac drives.

d-q EQUATIONS OF THE SYNCHRONOUS RELUCTANCE MACHINE

The equations which describe the behavior of the synchronous reluctance machine can be derived from the conventional equations depicting a conventional wound field synchronous machine, that is Park's Equations [4]. In synchronous reluctance machines, the excitation winding is non-existent. Also, in machines typically employing a modern axially laminated rotor structure, the rotor cage is normally omitted since the machine can be starting synchronously from rest by proper inverter control. Hence, elimination of both the field winding and damper winding equations from Park's equations forms the basis for the d-q Equations for a synchronous reluctance machine. That is,

$$v_{ds} = r_s i_{ds} + \frac{d}{dt}\lambda_{ds} - \omega_r \lambda_{qs} \quad (1)$$

$$v_{qs} = r_s i_{qs} + \frac{d}{dt}\lambda_{qs} + \omega_r \lambda_{ds} \quad (2)$$

$$\lambda_{ds} = L_{ls} i_{ds} + L_{md} i_{ds} \quad (3)$$

$$\lambda_{qs} = L_{ls} i_{qs} + L_{mq} i_{qs} \quad (4)$$

where L_{md}, L_{mq} and L_{ls} are, respectively, the direct axis and quadrature axis magnetizing inductances and the leakage inductance. The quantity r_s is the stator resistance per phase and ω_r is the speed of the rotor. In terms of the d-q variables, the electromagnetic torque is identical to that of a synchronous machine, namely,

$$T_e = \frac{3}{2}\frac{P}{2}(\lambda_{ds} i_{qs} - \lambda_{qs} i_{ds}) \quad (5)$$

The torque equation 5 can also be written in terms of stator d-q currents as

$$T_e = \frac{3}{2}\frac{P}{2}(L_{md} - L_{mq}) i_{ds} i_{qs} \quad (6)$$

where P is the number of poles.

The equations are simple compared to ones of synchronous or induction machines because the field winding is non-existent and a rotor cage is normally omitted, which predicts that the control scheme of the synchronous reluctance motors can be simpler than ones of synchronous or induction machines.

THE STEADY STATE EQUATIONS FOR A SYNCHRONOUS RELUCTANCE MACHINE

The d-q Eqs. 1-6 express the behavior of the physical stator currents in a reference frame which is rotating with the rotor of the machine in much the same manner as for a wound field synchronous machine (rotor reference frame). When balanced three phase voltages are applied to the machine, these voltages form a constant amplitude rotating vector in the d-q plane. When the rotor rotates at the same angular velocity as the angular velocity of the rotating voltage vector (modified by the number of pole pairs), the voltage vector appears to be stationary in the rotor reference frame. In this case it is conventional to describe the angular relationship between the stator voltage vector and the d-q axes as the two components

$$V_{qs} = V_s \cos\delta \quad (7)$$

$$V_{ds} = -V_s \sin\delta \quad (8)$$

When the d-q components of the stator voltage are constant, the "variables" in the differential Eqs. 1 and 2 also become constant in the steady state.

The currents can then be solved in terms of the steady state voltages as

$$I_{ds} = \frac{\omega_e L_{qs} V_{qs} + r_s V_{ds}}{r_s^2 + \omega_e^2 L_{ds} L_{qs}} \quad (9)$$

$$I_{qs} = \frac{-\omega_e L_{ds} V_{ds} + r_s V_{qs}}{r_s^2 + \omega_e^2 L_{ds} L_{qs}} \quad (10)$$

TORQUE EXPRESSIONS FOR CONSTANT VOLTS/HERTZ AND CONSTANT CURRENT OPERATION

Using Eqs. 9 and 10, the torque equation can be solved in terms of the voltage as

$$T_e = \frac{3}{2}\frac{P}{2}(L_{ds} - L_{qs})(-\omega_e L_{ds} r_s V_{ds}^2 + \omega_e L_{qs} r_s V_{qs}^2 + (r_s^2 - \omega_e^2 L_{ds} L_{qs}) V_{ds} V_{qs}) \frac{1}{(r_s^2 + \omega_e^2 L_{ds} L_{qs})^2} \quad (11)$$

At all but frequencies near zero, Eq. 11 is well approximated by neglecting the stator resistance, in which case Eq. 11 reduces to

$$T_e = -\frac{3}{2}\frac{P}{2}\frac{(L_{ds} - L_{qs})}{L_{ds} L_{qs}}\left(\frac{V_{ds}}{\omega_e}\right)\left(\frac{V_{qs}}{\omega_e}\right) \quad (12)$$

Substituting Eqs. 7 and 8 we obtain the torque in terms of the volts per hertz and "torque angle" δ as

$$T_e = \frac{3}{2}\frac{P}{2}\left[\frac{1}{L_{qs}} - \frac{1}{L_{ds}}\right]\left(\frac{V_s}{\omega_e}\right)^2 \frac{\sin 2\delta}{2} \quad (13)$$

Hence, the torque varies at the square of the volts per hertz and as the sine of twice the angle δ. When the volts per hertz is fixed, the maximum torque is clearly reached when $\delta = 45°$ at which point

$$T_{e(max)} = \frac{3}{4}\frac{P}{2}\left[\frac{1}{L_{qs}} - \frac{1}{L_{ds}}\right]\left(\frac{V_s}{\omega_e}\right)^2 \quad (14)$$

The presence of the "1/2" term on the right hand side Eq. 13 is frequently used as a justification for claiming that the synchronous reluctance motor is a poor torque producer. That this is not necessarily the case will be demonstrated in the next section.

The steady state torque can also be written in terms of stator d-q currents as

$$T_e = \frac{3}{2}\frac{P}{2}(L_{ds} - L_{qs})\, I_{ds}\, I_{qs} \quad (15)$$

Clearly the currents, as described by Eqs. 9 and 10 also describe a constant amplitude vector on the d-q plane. If we write the solutions to these equations as

$$I_{ds} = I_s \cos\varepsilon \quad (16)$$

$$I_{qs} = I_s \sin\varepsilon \quad (17)$$

then the electromagnetic torque can be expressed in terms of the stator current amplitude and "MMF angle" ε as

$$T_e = \frac{3}{2}\frac{P}{2}(L_{ds} - L_{qs})\, I_s^2 \frac{\sin 2\varepsilon}{2} \quad (18)$$

Note the great similarity of this expression to Eq. 13. The torque is thus also proportional to the square of the stator current and the sine of twice the MMF angle ε. Figures 1 and 2 show the "torque vs. angle" curves for both constant volts per hertz operation and for constant current operation. Also plotted is the corresponding variation of the angles δ and ε for case $L_{ds}/L_{qs} = 8.0$.

MAXIMUM POWER FACTOR

A frequently used argument against the use of a synchronous reluctance motor is its "poor" power factor. It is useful to consider this issue more closely. The power factor of a synchronous reluctance motor, $\cos\phi$, can be expressed as the ratio of the projection of the voltage vector on the current vector divided by the amplitude of the voltage vector. That is,

$$\cos\phi = \frac{V_{qs}\sin\varepsilon + V_{ds}\cos\varepsilon}{\sqrt{V_{qs}^2 + V_{ds}^2}} \quad (19)$$

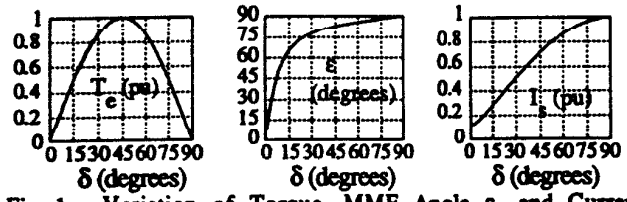

Fig. 1 Variation of Torque, MMF Angle ε, and Current Amplitude as a Function of δ for Constant Volts/Hz Operation, $L_{ds}/L_{qs} = 8.0$.

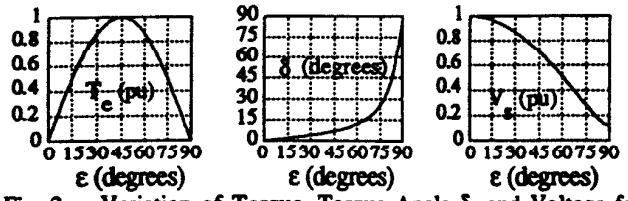

Fig. 2 Variation of Torque, Torque Angle δ, and Voltage for Constant Current Operation, $L_{ds}/L_{qs} = 8.0$.

where V_{ds} and V_{qs} are the d- and q-axis steady state voltage in the rotating reference frame, and ε is the "MMF angle".

It is useful to determine which value of MMF angle results in the maximum power factor. If this point is chosen as the "rated" value then the machine can be considered as optimally performing its energy conversion function. It can be shown [5, 6] that the power factor reaches a maximum value of

$$\cos\phi_{max} = \frac{\kappa - 1}{\kappa + 1} k_{\phi max} \quad (20)$$

when the MMF angle reaches

$$\tan\varepsilon = \sqrt{\kappa}\left(\sqrt{1 + \frac{r_s^2}{X_{ds}X_{qs}}} + \sqrt{\frac{r_s^2}{X_{ds}X_{qs}}}\right) \quad (21)$$

where the quantity $k_{\phi max}$ is a constant which depends on the machine papameters, r_s, X_{ds}, and X_{qs}, and is 1 for the case where the stator resistance is neglected and about 1.1 for the case where the saliency ratio κ is 8 and r_s/X_{ds} is 0.05.

The motor power factor versus saliency ratio κ ($=L_{ds}/L_{qs}$) under maximum power factor control scheme is plotted in Figure 3, assuming that r_s/X_{ds} is 0.05. Note that for machines with a saliency ratio of 7, the power factor is near 0.8 which is not much poorer than that of a Class B induction machine rated about 10 HP.

The maximum power factor operation point is clearly an ideal operating condition for which to define rated torque.

CONDITIONS FOR CONSTANT STATOR FLUX

The torque of a synchronous reluctance machine can be controlled while maintaining either stator flux or air gap flux in much the same manner as an induction motor. However, in the field weakening range, when the voltage supply (i.e., the inverter) saturates, the voltage amplitude becomes constant and, except for the IR drop, the stator flux becomes fixed. Hence, it is simplest to develop a torque controller which ensures constant stator flux linkage. From Eq. 5 we have, for the electromagnetic torque,

$$T_e = \frac{3}{2}\frac{P}{2}(\lambda_{ds}\, i_{qs} - \lambda_{qs} i_{ds}) \quad (22)$$

From Fig. 4 it can be determined that

$$\lambda_{ds} = \lambda_s \cos\delta' \quad (23)$$

and

$$\lambda_{qs} = \lambda_s \sin\delta' \quad (24)$$

so that Eq. 22 can be written as

$$T_e = \frac{3}{2}\frac{P}{2}(\lambda_s \sin\delta'\, i_{qs} - \lambda_s \cos\delta'\, i_{ds}) \quad (25)$$

However, from Fig. 4, the component of stator current orthogonal to the stator flux vector λ_s is

$$i_{ts} = i_{qs}\sin\delta' - i_{ds}\cos\delta' \quad (26)$$

Hence, the torque equation of a synchronous reluctance motor can be written in alternative form as

$$T_e = \frac{3}{2}\frac{P}{2}\lambda_s\, i_{ts} \quad (27)$$

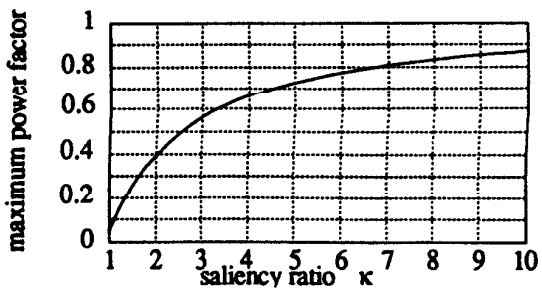

Fig. 3 Power factor vs. saliency ratio κ ($=L_{ds}/L_{qs}$) of a synchronous reluctance motor when the motor is controlled with the maximum power factor control scheme.

where

$$\lambda_s = \sqrt{\lambda_{ds}^2 + \lambda_{qs}^2} \quad (28)$$

$$\lambda_{ds} = L_{ds}\, i_{ds} \quad (29)$$

$$\lambda_{qs} = L_{qs}\, i_{qs} \quad (30)$$

$$i_{qs} = i_{ts}\cos\delta' + i_{fs}\sin\delta' \quad (31)$$

$$i_{ds} = -\, i_{ts}\sin\delta' + i_{fs}\cos\delta' \quad (32)$$

Since the stator current must be expressed in terms of two components, the companion component of stator current corresponding to the "torque component" of stator current i_{ts} has been defined as i_{fs}, i.e., the "flux" component of stator current. Rewriting Eqs. 23 and 24 using i_{ts}, i_{fs} and δ',

$$\lambda_s \cos\delta' = L_{ds}\, i_{ds} = L_{ds}\,(-\, i_{ts}\sin\delta' + i_{fs}\cos\delta') \quad (33)$$

$$\lambda_s \sin\delta' = L_{qs}\, i_{qs} = L_{qs}\,(i_{ts}\cos\delta' + i_{fs}\sin\delta') \quad (34)$$

Thus

$$\lambda_s = L_{ds}\,(-\, i_{ts}\tan\delta' + i_{fs}) \quad (35)$$

$$\lambda_s \tan\delta' = L_{qs}\,(i_{ts} + i_{fs}\tan\delta') \quad (36)$$

where

λ_s; stator flux linkage,

i_{ts}; torque producing current - peak value

i_{fs}; stator flux producing current - peak value

δ'; angle between stator flux linkage and rotor d-axis (identical to δ, the angle between the stator voltage vector and the rotor q-axis if the stator IR drop is neglected)

The torque current command i_{ts}^* is determined from the torque equation, Eq. 27, for given torque command T_e^* and air gap flux command λ_s^*.

$$i_{ts}^* = \frac{T_e^*}{\frac{3}{2}\frac{P}{2}\lambda_s^*} \quad (37)$$

From Eq. 35 the term $\tan\delta^*$ is expressed in terms of i_{ts}^* and i_{fs}^* and, by substituting $\tan\delta^*$ into Eq. 36,

$$\tan\delta^* = \frac{L_{ds}\, i_{fs}^* - \lambda_s^*}{L_{ds}\, i_{ts}^*} \quad (38)$$

$$\lambda_s^* \frac{L_{ds} i_{fs}^* - \lambda_s^*}{L_{ds} i_{ts}^*} = L_{qs}\, i_{ts}^* + L_{qs}\frac{L_{ds} i_{fs}^* - \lambda_s^*}{L_{ds}\, i_{ts}^*}\, i_{fs}^* \quad (39)$$

Solving for i_{fs}^*

$$i_{fs}^* = \frac{\lambda_s^*(L_{ds}+L_{qs}) - \sqrt{\lambda_s^{*2}(L_{ds}-L_{qs})^2 - (2L_{ds}L_{qs}i_{ts}^*)^2}}{2L_{ds}L_{qs}} \quad (40)$$

The necessary condition to have a real solution for i_{fs}^* is

$$\lambda_s^* > \frac{2L_{ds}L_{qs}i_{ts}^*}{(L_{ds}-L_{qs})} \quad (41)$$

Substituting Eq. 37 into Eq. 41, we can determine a restriction for the stator flux control scheme.

$$\lambda_s^* > \sqrt{\frac{2L_{ds}L_{qs}}{(L_{ds}-L_{qs})}\,\frac{T_e^*}{\frac{3}{2}\frac{P}{2}}} \quad (42)$$

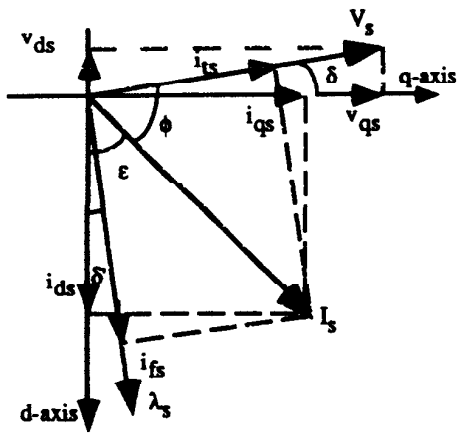

Fig. 4 d-q vector diagram for control of the stator flux linkage.

This restriction is, of course, always satisfied in the constant torque range for torque up to and including the rated value. However, the restriction becomes important when field weakening is employed.

FIELD WEAKENING CONTROL

The stator flux linkage at the base speed and under the rated (maximum power factor) condition is

$$\lambda_{s(base)}^* = \sqrt{[(L_{ds}\cos\varepsilon_{base})^2 + (L_{qs}\sin\varepsilon_{base})^2]\,(I_{s(base)}^*)^2} \quad (43)$$

Using Equation 18

$$I_{s(base)}^{*\,2} = \frac{T_{e(base)}^*}{\frac{3}{2}\frac{P}{2}(L_{ds}-L_{qs})}\,\frac{2}{\sin 2\varepsilon_{base}} \quad (44)$$

Substituting this result into Eq. 43

$$\lambda_{s(base)}^* = \sqrt{\left(L_{ds}^2\frac{\cos\varepsilon_{base}}{\sin\varepsilon_{base}} + L_{qs}^2\frac{\sin\varepsilon_{base}}{\cos\varepsilon_{base}}\right)\frac{T_{e(base)}^*}{\frac{3}{2}\frac{P}{2}(L_{ds}-L_{qs})}} \quad (45)$$

The stator flux linkage in the field weakening region

$$\lambda_s^* = \lambda_{s(base)}^*\frac{\omega_b}{\omega_e} = \frac{\omega_b}{\omega_e}\sqrt{\left(L_{ds}^2\frac{\cos\varepsilon_{base}}{\sin\varepsilon_{base}} + L_{qs}^2\frac{\sin\varepsilon_{base}}{\cos\varepsilon_{base}}\right)\frac{T_{e(base)}^*}{\frac{3}{2}\frac{P}{2}(L_{ds}-L_{qs})}} \quad (46)$$

Applying the restriction on stator flux, Eq. 42,

$$\lambda_s^* = \lambda_{s(base)}^*\frac{\omega_b}{\omega_e} > \sqrt{\frac{2L_{ds}L_{qs}}{(L_{ds}-L_{qs})}\,\frac{T_{e(base)}^*}{\frac{3}{2}\frac{P}{2}}\,\frac{\omega_b}{\omega_e}} \quad (47)$$

Equating Eqs. 45 and 47, the limitation of the field weakening range can be determined to be

$$\frac{\omega_e}{\omega_b} < \frac{L_{ds}^2\frac{\cos\varepsilon_{base}}{\sin\varepsilon_{base}} + L_{qs}^2\frac{\sin\varepsilon_{base}}{\cos\varepsilon_{base}}}{2L_{ds}L_{qs}} \quad (48)$$

Assume now that the rated condition is defined to be at the case where the power factor is a maximum. We have

$$\tan\varepsilon_{base} = \sqrt{\kappa} = \sqrt{\frac{L_{ds}}{L_{qs}}} \quad (49)$$

Substituting Eq. 49 into Eq. 48

$$\frac{\omega_e}{\omega_b} < \frac{1}{2}\left(\sqrt{\frac{L_{ds}}{L_{qs}}} + \sqrt{\frac{L_{qs}}{L_{ds}}}\right) \quad (50)$$

Hence, the equation defining the maximum field weakening range for constant stator flux is

$$\frac{\omega_{e(max)}}{\omega_b} = \frac{1}{2}\left(\sqrt{\kappa} + \sqrt{\frac{1}{\kappa}}\right) \quad (51)$$

where κ is the saliency ratio, L_{ds}/L_{qs}.

A sketch of the function of Eq. 51 is shown in Fig. 5. Note that a field weakening range of about 1.6 can be obtained when the saliency ratio is about 8.0.

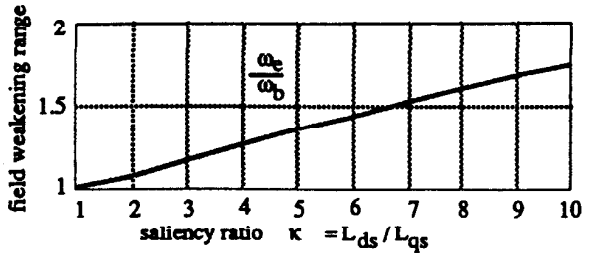

Fig. 5 Field weakening range ω_e/ω_b vs. saliency ratio κ when the stator flux control scheme is applied.

CURRENT VECTOR PROFILE VERSUS LOAD

At this point all of the necessary equations to discuss field oriented control of the synchronous reluctance machine have been derived. Consider first, the current versus load profile. It can be recalled that in the case of an induction motor, the rotor flux is held constant while the component of stator current flowing in the rotor resistor R_2/S is varied with the torque demand. In general, this is done due to the fact that the rotor flux producing component of stator current affects the torque very slowly due to the long rotor time constant. However, in the case of the synchronous reluctance machine, no rotor windings exist to oppose this flux producing component. Hence, the rotor flux can be changed much more rapidly (at least at low and moderate speed where good current regulation is possible). Hence, both the flux and torque producing components can be increased as desired to satisfy the torque and another criterion as well. In most cases the conductor losses of the machine will dominate in which case it would be desirable to minimize the conductor I^2R loss. It is obvious from Eq. 18 that the maximum torque per ampere is obtained by setting $\varepsilon = 45°$ in which case $I_{ds} = I_{qs}$. However, this strategy cannot be maintained as load continues to increase since at some point the flux established in the d-axis by I_{ds} begins to exceed the rated flux. Hence, when

$$I_{ds} X_{ds} = \omega_e \lambda_{rated} \tag{52}$$

the current I_{ds} must be maintained as constant while the q-axis component I_{qs} continues to increase to satisfy the load. The current I_{qs} continues to increase until rated load is reached (maximum power factor condition). At the maximum power factor point, I_{qs} is greater than I_{ds} by the factor,

$$I_{qs} = I_{ds} \sqrt{\frac{L_{ds}}{L_{qs}}} \tag{53}$$

When $\kappa = 8.0$ this factor is 2.8. Figure 6 shows the current versus load profile for the case of $\kappa = L_{ds}/L_{qs} = 8.0$.

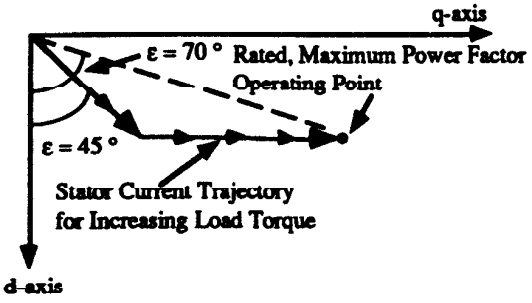

Fig. 6 Locus of the Stator Current Vector as a Function of Load, $\kappa = 8.0$.

CURRENT VECTOR PROFILE VERSUS SPEED

Although the locus of Fig. 6 always remains the desired locus for the stator current vector, it is not possible to remain on this optimum locus when insufficient voltage forcing exists to establish the required current. That is, when the inverter begins to saturate (i.e., enter "square wave" operation), the machine enters the field weakening mode in much the same manner as any ac or dc machine. Returning again to the two steady state equations for the d-q current, neglecting the effects of stator resistance,

$$V_s \cos\delta = X_{ds} I_{ds} \tag{54}$$

$$V_s \sin\delta = X_{qs} I_{qs} \tag{55}$$

Taking the sum of the squares of these two equations,

$$\frac{V_s^2}{X_{qs}^2} = \left(\frac{X_{ds}}{X_{qs}}\right)^2 I_{ds}^2 + I_{qs}^2 \tag{56}$$

Note that the right hand side of Eq. 56 is independent of the applied frequency ω_e while the left hand side varies since the amplitude of the voltage V_s and the q-axis reactance X_{qs} varies with frequency. When the machine operates in the constant torque mode, the machine essentially receives constant volts/hertz in which case the terminal voltage can be written in terms of the base voltage (maximum inverter output voltage) as

$$V_s = \frac{\omega_e}{\omega_{base}} V_{s(base)} \tag{57}$$

in which case Eq. 56 can be written as,

$$\frac{V_{s(base)}^2}{\omega_{base} L_{qs}^2} = \left(\frac{L_{ds}}{L_{qs}}\right)^2 I_{ds}^2 + I_{qs}^2 \tag{58}$$

Equation 58 clearly describes an ellipse on the d-q plane with its major axis on the q-axis equal to V_s/X_{qs} and minor axis on the d-axis equal to V_s/X_{ds}. If it is assumed that the voltage fundamental component available from the inverter is just sufficient to establish the rated current condition at the rated (base) frequency, then the ellipse described by Eqs. 58 also passes through the operating point for full (or maximum) load operation described by the point of Fig. 7 as shown in Fig. 7. When the frequency exceeds the base frequency, then the voltage V_s becomes constant at $V_{s(base)}$, while the reactance X_{qs} continues to increase. The ellipse becomes described by

$$\frac{1}{(\omega_e/\omega_{base})^2} \frac{V_{s(base)}^2}{(\omega_{base} L_{qs})^2} = \left(\frac{L_{ds}}{L_{qs}}\right)^2 I_{ds}^2 + I_{qs}^2 \tag{59}$$

Hence, the size of the ellipse begins to decrease inversely with the square of the frequency ratio ω_e/ω_{base}. In this case the rated current condition cannot be established but is forced to remain on the ellipse. Assuming that the maximum current amplitude must remain fixed at the value defined by the base or rated condition fixes the range of operation on the ellipse for any frequency. Figure 7 also shows a second ellipse for the case where the frequency ratio $\omega_e/\omega_{base} = 1.1$.

In Fig. 8(a) shown are the limiting values of d- and q-axis stator current set by the shrinking ellipse as speed increases beyond base speed. In this case the maximum current for each speed was chosen as that value which will produce rated power. Figure 8(b) shows the resulting torque and power profiles versus speed when, again, $\kappa = 8.0$, which clearly demonstrates the required constant torque and constant power regions of operation. Figure 8(c) shows the variation of the stator flux which is first constant over the constant torque

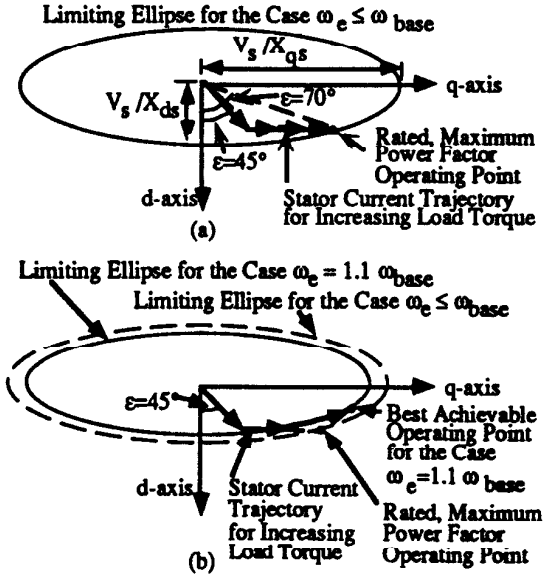

Fig. 7 Showing elliptical boundaries for the current vector I_s for the cases a) $\omega_e \le \omega_{base}$ and b) $\omega_e = 1.1\ \omega_{base}$.

range of operation and then decreases inversely with speed when the power becomes constant. With a saliency ratio of 8.0 the constant power region can be extended to 1.6 per unit speed. Larger speed ranges are, of course, possible but at the expense of reducing the base torque which, in turn, penalizes the machine because of the poorer power factor.

In Figs. 8(d) and (e) shown are the corresponding stator current and voltage. As necessary, the stator voltage becomes constant during the constant power mode while the stator current is constant during the constant torque mode. As the power factor rapidly changes during the constant power mode, the stator current cannot remain constant but increases until the motor reaches the pullout point ($\delta = 45°$).

In Fig. 8(f) and (g) shown are the variation of the MMF angle ε and the torque angle δ' over the constant torque and constant power regions. In Fig. 8(h) the power factor of the machine is shown as a function of speed. Note that the power factor rapidly decreases when the machine enters the constant power region as the torque angle δ' begins to approach 45°.

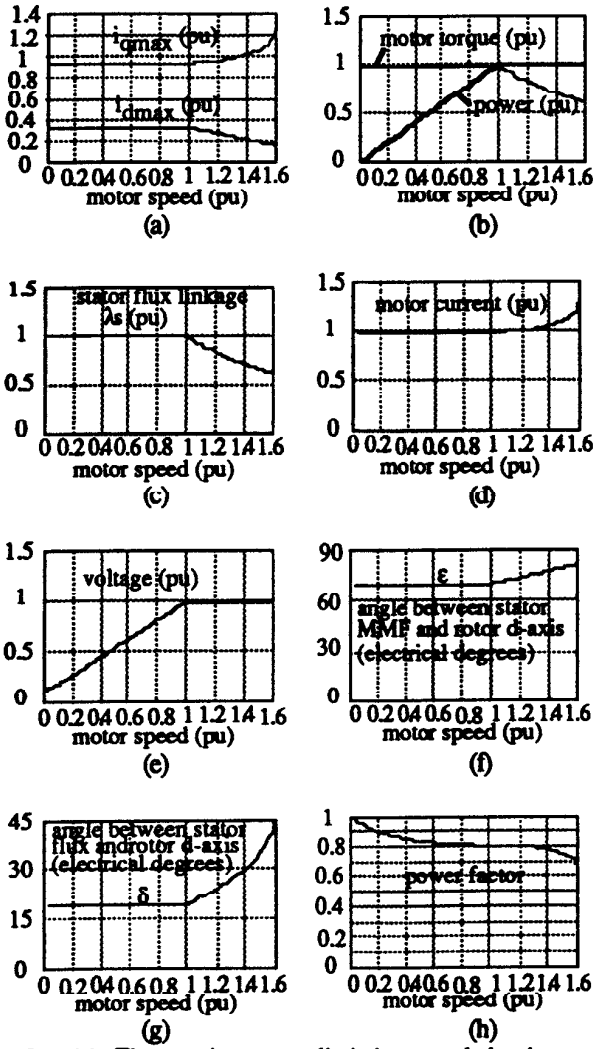

Fig. 8 (a): The q-axis current limit i_{qmax} and d-axis current limit i_{dmax} vs. motor speed, (b): the motor torque and power vs. motor speed, (c): the stator flux linkage λ_s vs. motor speed, (d): the motor current vs. motor speed, and (e): the motor voltage vs. motor speed, (f): the angle between stator MMF and rotor d-axis vs. motor speed, (g): the angle between stator flux and rotor d-axis vs. motor speed, and (h): Power factor vs. motor speed, which are calculated based on the stator flux control scheme, $\kappa = 8.0$.

BLOCK DIAGRAM FOR IMPLEMENTING FIELD ORIENTED CONTROLLER

Figure 9 shows the overall control strategy for controlling torque and speed of a synchronous reluctance motor. By means of an absolute encoder or resolver, the sine and cosine of the angular position of the rotor is established. These sinusoidal components are used to refer those physical stator currents from the physical (stationary) reference frame to the rotating (d-q) axes. The encoder is also used to measure speed and, based on the speed measurement, the desired (command) values of i_{ds} and i_{qs} are established. Current regulators guarantee that the desired and actual values of the d-q currents are obtained. The voltage command signals which are obtained in the synchronously rotating d-q frame are finally referred back to the stator frame before being used to switch the voltage source PWM inverter.

Figure 10 shows a more detailed block diagram indicating several of the practical features used to improve the performance of such a motor drive. In particular, blocks indicating a "feedforward" type of speed invariant current controller, a d- and q-axis current limiter and a variable gain speed regulator are shown. The exact nature of the speed invariant current control block is explained in Figure 11.

Referring back to "Park's Equations" for a synchronous reluctance machine, Eqs. 1 and 2, the presence of the "counter emf terms" $\omega_r\lambda_{ds}$ and $\omega_r\lambda_{qs}$ can be recalled. When speed changes rapidly, these terms cause a slew rate error in the current regulator since the integrators of the two PI current controllers must continually slew upward at a rate proportional to speed due to the cemf terms in addition to performing their function of regulating the two components of stator current. This requirement can be eliminated by supplying the counter emf portion of the applied voltage separately by means of feedforward control as shown in Fig. 11. In this figure, the speed voltage components $\omega_r\lambda_{ds} = \omega_r L_{ds} I_{ds}$, and $\omega_r\lambda_{qs} = \omega_r L_{qs} I_{qs}$ are formed by looking up the inductances L_{ds} and L_{qs} as functions of I_{ds} and I_{qs} from a lookup table, forming $L_{ds}I_{ds}$ and $L_{qs}I_{qs}$, multiplying these results by ω_r and, finally, appropriately adding these quantities to the outputs of the current regulators, V_{qs}^* and V_{ds}^* to form the applied voltages in the d-q frame, V_{qs}^* and V_{ds}^*. By utilizing the output of the position encoder, these voltage command signals are finally transformed from the synchronous to the stationary reference to form the actual switching commands of the inverter.

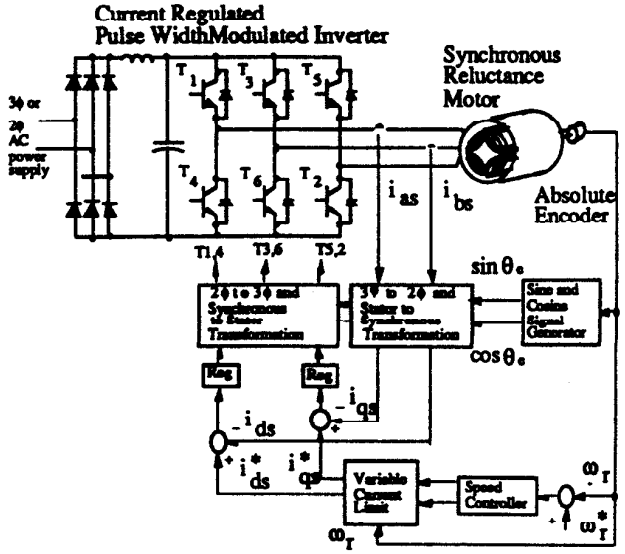

Fig. 9 General control configuration for a synchronous reluctance motor drive.

The d- and q-axis current limiter of Fig. 10 is shown in more detail in Fig. 12. These permitted maximum values are essentially the same ones as calculated in Fig. 8.

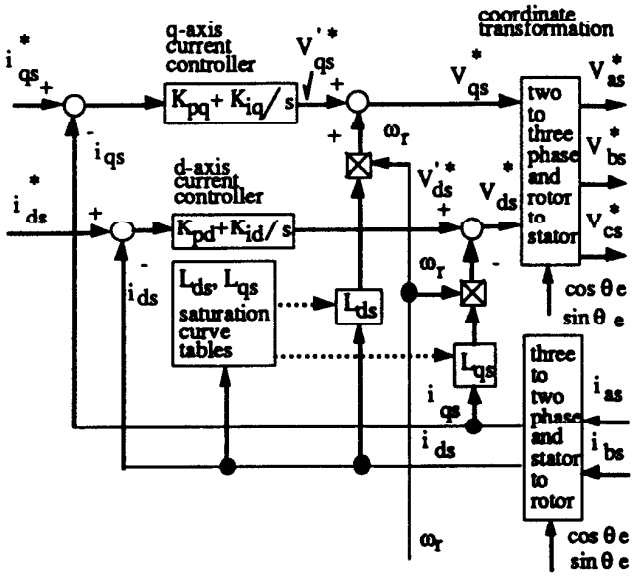

Fig. 11 Details of the rotor speed invariant d-q current regulator for synchronous reluctance motor drive considering also effects of saturation on L_{ds} and L_{qs}.

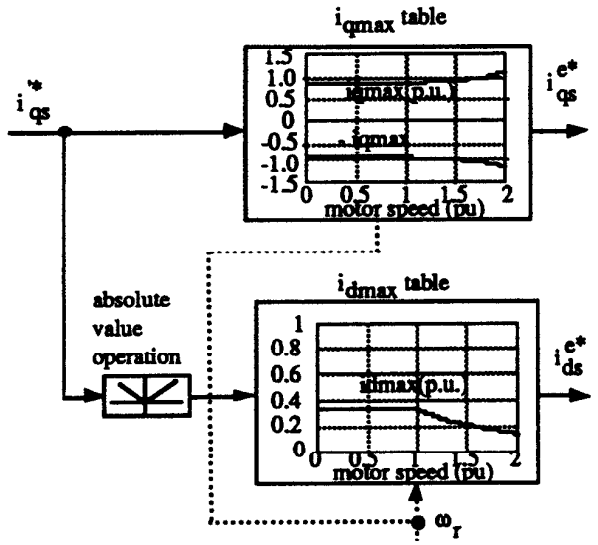

Fig. 12 Details of the variable d-q current limit functional blocks.

The details of the variable gain block are revealed in Fig. 13. Since torque is proportional to the product of d-axis times q-axis stator current (Eq. 6), so that when i_{ds} varies as a function of i_{qs}^*, the gain between the torque command and the q-axis current command effectively changes. This effect can be compensated by the use of a divider and multiplier which increases the gain block to compensate for the decreased gain due to reduction in i_{ds}.

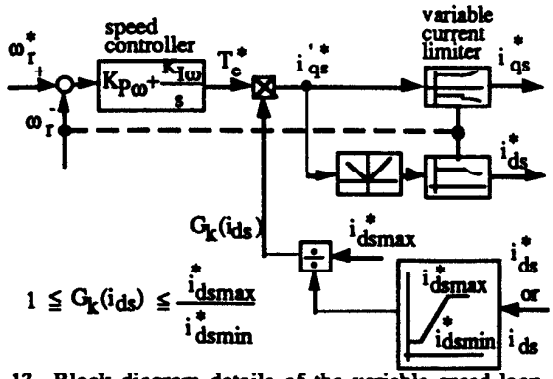

Fig. 13 Block diagram details of the variable speed loop gain function.

EXPERIMENTAL RESULTS

A synchronous reluctance motor drive with the field oriented control discussed in this paper has been implemented in the laboratory in order to study the performance of the proposed control schemes. All the control functions are implemented with software and a conventional transistor inverter was used to drive the motor. The experimental synchronous reluctance motor [6] was used, which has a saliency ratio L_{ds}/L_{qs} of 6.7 for the unsaturated conditions and 6.4 for the saturated conditions, and almost no cross coupling effects on both d- and q-axis magnetizing inductances.

Figure 14 and 15 show the experimental results of the d- and q-axis current step responses indicating the effect of the speed invariant current controller. In particular, the q-axis current control has significantly been improved with the function. The speed step response is shown in Fig. 16 where the current control scheme is clearly shown. The d-axis current is limited at a specified level while the q-axis current is increased to produce the required torque. Figure 17 shows four quadrant operation of the motor with the field weakening control where the base speed is 1300 rpm and the top speed is 2080 rpm.

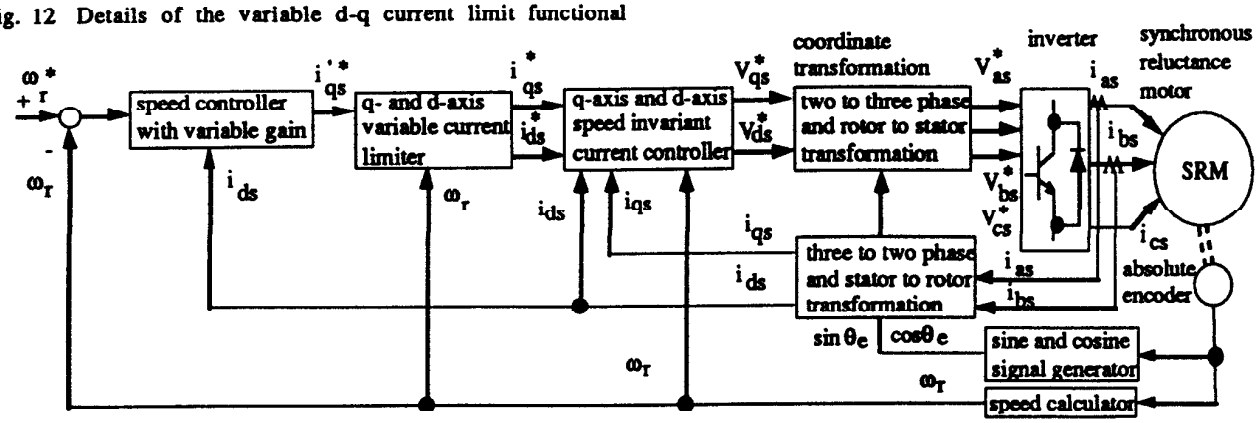

Fig. 10 More detailed control block diagram of synchronous reluctance motor drive system showing variable speed gain and decoupler in the current regulator.

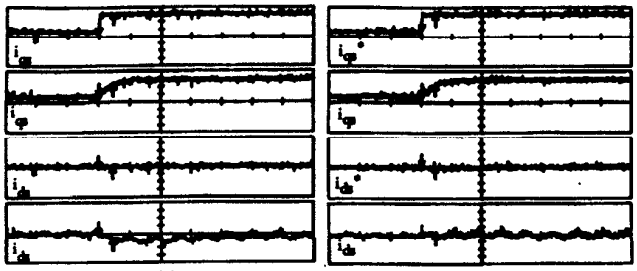

(a) (b)

Fig. 14 d-axis current step response at 600 rpm, (a): without and (b): with the speed invariant current controller. From top to bottom for both figures: (i) d-axis current command i_{ds}^* (1.6 A/div.), (ii) d-axis current i_{ds} (1.6 A/div.), (iii) the q-axis current command i_{qs}^* (1.6 A/div.), (iv) the q-axis current i_{qs} (1.6 A/div.), and the time scale is 0.01 sec./div..

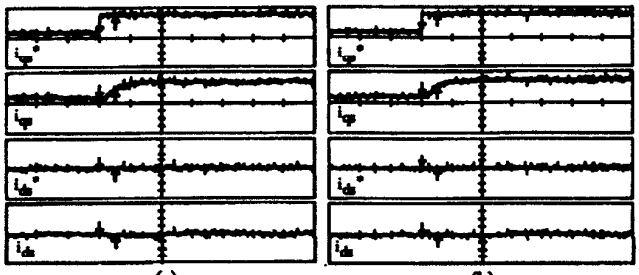

(a) (b)

Fig. 15 q-axis current step response at 600 rpm, (a): without and (b): with the speed invariant current controller. From top to bottom for both figures: (i) q-axis current command i_{qs}^* (1.6 A/div.), (ii) q-axis current i_{qs} (1.6 A/div.), (iii) the d-axis current command i_{ds}^* (1.6 A/div.), (iv) the d-axis current i_{ds} (1.6 A/div.), and the time scale is 0.01 sec./div..

CONCLUSIONS

In this work, control strategies, practical implementation and performance of a field oriented control of synchronous reluctance motors have been presented. A field oriented control scheme with a speed invariant current controller, a variable d-q current limit and a variable speed loop gain for synchronous reluctance motors is proposed. The relationship between the field weakening range and the saliency ratio is clearly derived in this paper. Excellent control performance has been obtained, which indicates that although there exists a limitation on the field weakening range, the synchronous reluctance motors can be suitably applied to high performance drive systems.

ACKNOWLEDGMENT

The authors are grateful to Gary E. Horst of Emerson Electric Co., St. Louis for fabricating the experimental synchronous reluctance motor

REFERENCES

[1] J. K. Kostko, "Polyphase Reaction Synchronous Motors", Journal of American Institute of Electrical Engineers, 1923, 42, pp. 1162-1168.

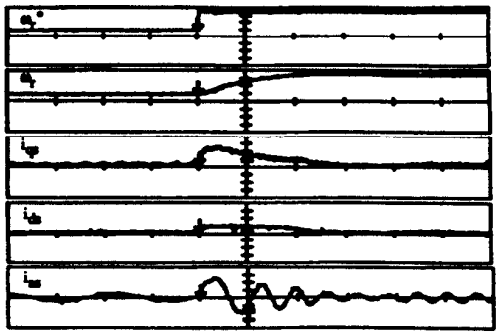

Fig. 16 Speed step response from 130 rpm to 520 rpm. From top to bottom: (i) the speed reference (167 rpm/div.), (ii) the rotor shaft speed (167 rpm/div.), (iii) the q-axis current (1.6 A/div.), (iv) the d-axis current (1.6 A/div.), (v) the motor phase current (1.6 A/div.), and the time scale is 0.1 sec./div..

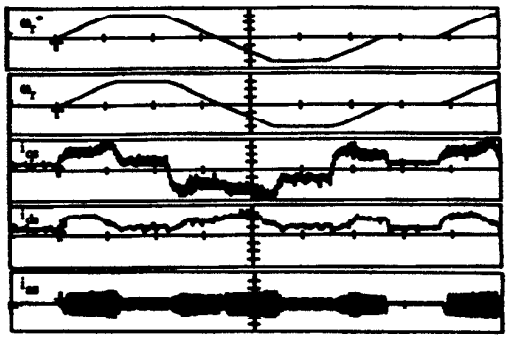

Fig. 17 Four quadrant operation with the field weakening control where the base speed is 1300 rpm and the top speed is 2080 rpm. From top to bottom: (i) the speed reference (666 rpm/div.), (ii) the rotor shaft speed (666 rpm/div.), (iii) the q-axis current (0.64 A/div.), (iv) the d-axis current (0.64 A/div.), (v) the motor phase current (1.6 A/div.), and the time scale is 2 sec./div..

[2] P.J. Lawrenson and L.A. Agu, "Theory and Performance of Polyphase Reluctance Machines", IEE Proc., vol. 111, No. 8, August 1964, pp. 1435-1445.

[3] T.A. Lipo,"Synchronous Reluctance Machines - A Viable Alternative for AC Drives?" Electric Machines and Power Systems, vol 19, pp. 659-671, 1991.

[4] R. H. Park, "Two-Reaction Theory of Synchronous Machines-II", AIEE Transactions, June 1933.

[5] T. A. Lipo and T. Matsuo "Synchronous Reluctance Motors and Drives - A New Alternative. Section 1 - Performance of Synchronous Reluctance Motor Drive", Tutorial Notes, IEEE Annual Meeting, Octorber 1992.

[6] T. Matsuo and T. A. Lipo, "Rotor Design Optimization of Synchronous Reluctance Machine", IEEE Power Engineering Summer Meeting. July 1993. in progress.